# AVVAM-1 and Tank Vulnerability Sensitivity Studies

Dr. Donald F. Haskell
Vulnerability Laboratory
Ballistic Research Laboratories
Aberdeen Proving Ground, Maryland

## Introduction

AVVAM-1 (Armored Vehicle Vulnerability Analysis Model - first version) is a conceptual model and associated digital computer code recently developed (1) at the Ballistic Research Laboratories to analytically assess the vulnerability of all types of combat vehicles to hostile conventional weapons. It is applicable to combat vehicles in general including tanks, armored personnel carriers, armored reconnaissance vehicles, etc. AVVAM-1 is another step in the continuing vulnerability methodology development which has been pursued at BRL since tank vulnerability work was initiated at the Laboratories in 1950.

Early effort in the 1950's took the form of an extensive test firing program. Guided by the results of these tests, a method to evaluate the terminal effects of antitank warheads against tanks evolved in the late 1950's. This work originated the "damage concentration" concept and showed that a relationship exists between armor distribution, projectile perforation characteristics, and component kill probability. A "kill" is defined in terms of functional loss with the types of "kill" classified as follows:

M Kill: Loss of mobility
F Kill: Loss of firepower
M or F Kill: Loss of either mobility or firepower
K Kill: Complete loss of vehicle (vehicle damaged beyond repair).

As initially developed, the methodology utilized engineering drawings to determine the tank components (including crew personnel) that a projectile would encounter in passing through the target tank. Using this information, along with perforation and damage data from the tank tests, quantitative tank vulnerability in terms of probability of achieving a specific type of "kill" was calculated. To apply this method, called the "compartment kill" method, required laborious and time consuming hand calculations.

In the middle 1960's a significant step forward in the calculation of tank vulnerability to conventional hostile weapons was made when the "compartment kill" method was computerized. A combinatorial geometry technique was utilized to describe the tank target in terms acceptable to a high speed digital computer. By this technique the complex tank target is represented mathematically by a set of simple geometric shapes, or stated more precisely, by the locations and shapes of the various physical regions of the target in terms of the intersections and unions of the volumes contained in a set of simple geometric bodies. By employing this technique for describing the tank, together

with a computerized version of the basic vulnerability assessment method and hostile weapon dispersion data the "compartment kill" methodology was made suitable for use on a high speed digital computer. This methodology has seen extensive use since its development.

However, over the years since the time of the first extensive tank tests which form the foundation of the "compartment kill" methodology, various and significant changes in tank design have occurred. Advances have been made in firepower, mobility and protection. Some of these advances include stabilized fire control and gun systems, variable height hydropneumatic suspension systems, new engine transmissions, night vision devices, new and improved armor, and increased system sophistication in general. Not only have improvements in systems occurred but, in addition, the physical location of various components has changed. Consequently, these changes warranted the development of an improved tank vulnerability methodology that could account for the influence of the individual components. For this reason, among others, and to provide improved guidance in the combat vehicle design process, AVVAM-1 was developed.

Effort was started on AVVAM in June 1972 and the first version, AVVAM-1, was made available in February 1973. The new code is ideal for both armored vehicle vulnerability and antiarmor weapons design and analysis studies. This first version of AVVAM treats components and personnel subjected to penetration and/or perforation damage mechanisms. The attacking munition may be a shaped charge or kinetic energy projectile, or a shaped charge or Misznay-Schardin land mine. With additional effort the present model may be extended to include other damage mechanisms as well. Although originally developed for armored vehicles, the code is not restricted to armored vehicles - it may be employed to assess the vulnerability of any materiel.

AVVAM-1 is based on analytical evaluations of the damage inflicted on individual critical components and the aggregate effect of these damaged components on compartment and overall vehicle vulnerability. To do this, AVVAM-1 accounts for not only the damage inflicted on components in the direct line of fire (shotline) of the attacking munition but also the damage inflicted by armor spall and/or munition fragment sprays on components located away from the munition shotline. AVVAM-1 also accounts for the degrading (or possibly enhancing) effects on the spall and/or fragment sprays caused by components positioned between the armor and the critical components. Thus, the potential protection afforded critical components by intervening components is included in the AVVAM-1 calculational procedure, and so, the effect of intervening components in reducing, or increasing the vulnerability, of a target vehicle may be evaluated by using AVVAM-1.

The code actually consists of two major, individual codes. One code is concerned with the vehicle geometry and configuration and the components in the vehicle critical to its operation. The other code is concerned with the terminal ballistics and behind-the-armor effects of the attacking munition as well as the assessment of kill probability. These two major code divisions are physically separated. The vehicle description and critical component location and description functions

are performed by one code, while the munition-target interaction characterization and kill probability assessment functions are performed by another code. Separation of these functions in this manner facilitates design optimization and systems analyses studies. Target vehicle parameters and/or munition parameters can be varied with relative ease. A series of munition design iterations or whole weapons systems intended to defeat a given target vehicle can be processed and evaluated by AVVAM-1 to achieve an optimum design. On the other hand, a similar iteration process can be followed in the optimum design of an armored vehicle. In this latter process a whole variety of armor materials and configurations as well as internal components and their character, configurations, and locations may be processed and evaluated until an optimum combination is achieved that provides the required degree of invulnerability to the attacking munition.

AVVAM development is not expected to halt with the first version described herein. On the contrary, a continuing extension, improvement and validation process is envisioned to provide the most accurate, efficient and reasonable armored vehicle vulnerability analysis tool possible.

Description of AVVAM-1

As described previously, AVVAM-1 is composed of two major computer codes. One of these characterizes the target. The other code characterizes the munition-target interaction and performs the vulnerability evaluation. The target characterization code describes the target and identifies, locates and determines the presented area of critical components. It also provides information concerning components that are located between the vehicle armor and critical components.

To generate the target description information, AVVAM-1 employs the GIFT (Geometric Information For a Target) code. This GIFT code is an improved version of the existing MAGIC code (2). It is presently being documented. The identification, location and presented area determinations of critical components and the intervening component information is generated by a new subcode recently developed at BRL called RIP (Rays Initiated at a Point).

The second major code employed in AVVAM-1 encompasses the terminal ballistics of the attacking munition and the post-plate-perforation characteristics of plate spall or munition fragment sprays. In addition, this second code calculates the vulnerability of selected components within the vehicle as well as compartment vulnerability and overall vehicle vulnerability. The code was also recently developed at BRL. Because of its functions, it is called the $P^3$ and the $C^3PKH$ (Post-Plate-Perforation and Component, Compartment and Combat Vehicle Probability of a Kill give a Hit) code.

In operation, AVVAM-1 selects critical components within the target and then evaluates the extent of damage and kill probability for each selected munition aimpoint in a given view of the target. It does this by determining the armor thickness in the direction of the attacking shotline of the munition, the number of interceding components between the vehicle armor and the critical component and then utilizes the behind-

the-plate characterization of a specific munition to calculate maximum, mean, and minimum kill probabilities given a hit for all or selected critical components within the vehicle. This whole process is accomplished by firing a selected number of parallel rays at a given attack angle and azimuth into the target. Each individual parallel ray then spawns new rays that are initiated at the munition exit point on the armor interior surface. These new rays are used to search out the vulnerable components, define their position, shielding, and presented area. Then the post-plate-perforation subcode, converts terminal ballistics input data into an expected number of hits into each of the vulnerable components and finally the $C^3PKH$ subcode determines the probability of a kill of these components for the expected number of hits. The kill probabilities for all the vulnerable components within a given compartment are combined into compartment M, F, & K kills. In addition, overall values for M, F, & K kills of the whole vehicle are also determined.

A flow chart summarizing the operations of AVVAM-1 is presented by FIG. 1. In this figure Box 1 represents the target input. Box 2 is the RIP section, Box 3 is the $P^3$ section and Box 4 is the $C^3PKH$ section. The $C^3PKH$ section provides the output in terms of probability of a kill given a hit. Also indicated in the figure is Box 5 which indicates an iteration scheme that may be employed for multiple views. Since the sections represented by Box 1, 2, 3, and 4 provide the PK/H output for a single view, results for multiple views may be obtained by iterating between Boxes 2, 3, and 4 for each view desired.

The code operates as follows: The particular target description is entered through Box 1 on cards and the specific munition is inputed by cards through Box 3. Information for the $P^3$ section is handled by card input. After the target is described and the critical components identified, RIP then, for a single vehicle view, selects a starting point on the vehicle, fires a main ray at the starting point, and essentially determines the position, shielding, and presented area of all the critical components in the vehicle in relation to the shotline of the main ray. The $C^3PKH$ code calls on the Post-Plate-Perforation code to supply the behind the plate spall data and main munition shotline information to include number of fragments, size, and speed of fragments. Next, it calculates the expected number of fragments to hit a given critical component and then the probability of killing that component given a hit. It does this for each critical component identified by the RIP code for the particular shotline selected. All the critical components are evaluated for the first shotline. The RIP code then moves to a new shotline (or shotpoint) and the maximum, mean, and the minimum probabilities of a kill given a hit are calculated for all the components in the view of the new shotline. This process is continued until the whole view of the vehicle is completed. At this point the output of the AVVAM code is the following: Maximum, mean, and minimum probability of a kill for each critical component in the vehicle, a set of compartment M, F, & K kill probabilities and overall vehicle view probability of M, F, & K kill values. During these calculations the $C^3PKH$ code in conjunction with the $P^3$ code account for the mass and velocity attrition of the shotline and spall fragments as they perforate intercedent components between the exit point on the armor and the specific vulnerable component under evaluation at that time.

## Description of Sensitivity Study

There are an abundance of variables in the attacking projectile-tank vulnerability analysis problem. These may be grouped into projectile, tank and model variables. For a specific projectile, a shaped charge projectile for example, the following noninclusive factors affect the terminal ballistic and behind-the-armor characteristics of the projectile:

liner cone material
liner cone base diameter
liner cone configuration
explosive weight
standoff
striking velocity
striking angle of obliquity

The characteristics that these factors affect include the following eight variables:

armor depth of penetration
spall cone axis-jet axis angle
fragment number spatial distribution
fragment mass spatial distribution
fragment speed spatial distribution
fragment mass-number distribution
fragment speed-mass distribution
fragment configuration.

Now, for purposes of this dicussion, the tank variables may be subdivided into armor variables and other-than-armor variables. The armor characteristics depend upon its fabrication technique (either rolled or cast) and its configuration. In the configuration category may be placed homogeneous armor and spaced armor. Homogeneous armor variables are: The material of construction (steel, aluminum, etc.) and thickness of the armor. Additional variables pertaining to spaced armor arrays include the number of plates in the configuration and their spacing (as well as material of construction and thicknesses). In the other-than-armor category are the character of the tank components and their location outside or inside the vehicle. Component placement is a function of the imagination of the designer. The variables that effect the character of the components are: their conditional probability for various kill categories, their equivalent steel thickness, and their contribution to overall tank kill catagories. Consequently, the number of tank variables is at least fourteen to sixteen.

Additional variables that play a big role in the application of AVVAM-1 concern the mathematical representation of the tank's geometry and configuration. These variables include (as a minimum) the following: the detail to which the tank is to be analyzed, the number of views of the tank to be evaluated, the overall grid size (or number of analytical firings into a particular view of the tank), and the number of rays fired at each critical component to delineate its shape, location, and shielding.

All this means that a relatively complete sensitivity study of tank vulnerability to a specific projectile type would essentially require an infinite number of variations. For economy the present study is concerned with a total of five variables. Three of these affect both projectile and armor behavior. The other two effect the tank behavior itself. The projectile type studied is the shaped charge. The factors studied that effect both the projectile and tank behavior are: average fragment number, average fragment mass, and average fragment speed. The tank variables studied are component conditional probability for a specific kill category and component equivalent steel thickness. A total of sixteen combinations of these variables were selected for study.

The object of this study is to illustrate, by an investigation of a limited set of parameters, typical results that may be obtained by employing AVVAM-1 in an operational analysis or systems effectiveness study for systems acquisition decisions.

## Results and Discussion

Figures 2 through 6 illustrate the trends in some of the results of the study. It should be emphasized here that these results correspond to a single, specific tank design and should not, at this time, be generalized. More work needs to be accomplished before generalizations could possible by made. However, a knowledge of the present results should be instructive. In all these figures normalized kill probability, $\bar{P}_k$, is plotted versus the various variables studied. Here, normalized kill probability relates the kill probability for a given set of values of the variables to the highest kill probability calculated i.e., the worst case condition for the tank considered in the study. Furthermore, the abscissas of these figures represent normalized values of the independent variables. This means that all the independent variables are presented relative to a given set of basic values of these variables. This basic value set corresponds to the present tank design and the behind-the-armor spall caused by a typical antitank shaped charge projectile. In the figures the baseline spall condition used as the norm for the various calculations is represented by N, M, and S. N, M, and S are respectively the total average number, average mass and average speed of the spall fragments produced behind the basic armor configuration by the baseline shaped charge munition. ET represents the baseline set of tank component equivalent steel thicknesses. Component equivalent steel thickness is a measure of the ballistic shielding provided by a tank component. The higher this value the harder it is for a spall fragment to perforate the component. PKH is used to represent the baseline set of component conditional kill probability values.

The influence of fragment mass on kill probability is illustrated by Fig. 2. The curve in this figure corresponds to the case in which the speed and number of fragments, component equivalent steel thickness, and component conditional kill probability set are maintained constant at the baseline values of S, N, ET and PKH, respectively. As indicated by the figure (and as to be expected) the normalized kill probability increases with increase in fragment mass. The curve is quite steep for $\bar{M}$ below 4 to 10 and begins to level off beyond $\bar{M}$ = 10 to 20. $\bar{P}_k$ increases

approximately 65% as the normalized fragment mass increases from 1 to 10. Although at $\bar{M} = 10$ a tenfold increase in $\bar{M}$ only yields about a 20% $\bar{P}_k$ increase.

Figure 3 shows the variation in normalized kill probability with normalized number of fragments. Component equivalent steel thickness and component conditional kill probability remain constant in all four curves shown. Curve A corresponds to the baseline fragment mass (M) and speed (S) while curve B corresponds to the same values of the variables as in A but with four times the baseline fragment mass (4M). Curve C corresponds to the same values of the variables as in A except the fragment speed is four times that of A (4S). Curve D is drawn for both four times the fragment mass (4M) and four times the fragment speed (4S) of curve A. Again, like the variation in kill probability with fragment mass illustrated by Fig. 2, Fig. 3 shows that kill probability increases with the number of fragments produced behind the armor. This increase, 42% for the baseline case of curve A from $\bar{N} = 1$ to 4, is the same as the $\bar{P}_k$ increase with normalized fragment mass shown by Fig. 2. In Fig. 2 fragment number is kept constant at $\bar{N}$ while the normalized fragment mass is varied, and from $\bar{M} = 1$ to 4 the $\bar{P}_k$ increase is 42%.

Figure 3 also illustrates the relative influence of fragment mass and speed. By comparing curves B and C with curve A, it is seen that behind-the-armor fragments with four times the speed of the baseline case result in a higher normalized kill probability than fragments of the same speed as the baseline case but with four times the mass. Curve C, which shows the effect of higher speed, ranges from $\bar{P}_k$ equal to 74% to 32% higher than the baseline case of curve A while curve B, which represents the effect of higher fragment mass only ranges from 42% to 23% higher than curve A. This shows that the influence of fragment speed on kill probability is greater than is the influence of fragment mass. This situation is to be expected particularly if tank kill probability were a direct function of fragment kinetic energy. However, the effect of fragment speed (over the range studied) is only 1.4 to 1.75 times greater than the effect of fragment mass. This is much less than the factor of 5 which would result if tank kill probability were a direct function of kinetic energy. Even so, this means that tank armor with the ability to limit fragment speed more than fragment mass should be more effective in achieving a lower overall tank kill probability than armor designed more toward limiting fragment mass.

The effect of an equal (fourfold) increase in both fragment mass and speed is illustrated by curve D of Fig. 3. In this case the figure shows that the number of fragments exerts little influence on $P_k$. A fourfold increase in the number of fragments only yields a 7% increase in $\bar{P}_k$. This condition is probably dependent upon the existence of a minimum, or threshold, number of fragments. Below this threshold number kill probability most likely decreases rapidly with decreasing numbers of fragments.

Figure 4 clearly illustrates the influence of normalized fragment speed on normalized kill probability for two cases. The upper curve corresponds to baseline case values of fragment number and mass, component equivalent steel thickness and component conditional kill probabili The lower curve corresponds to these same constant parameter values except the component equivalent steel thickness is double the upper curve. As indicated, tank kill probability increases significantly with fragment speed. This increase is 74% for the upper curve and 119% for the lower curve over an increase in $\bar{S}$ from 1 to 4. Fig. 4 also demonstrates that an increase in fragment speed can be offset to a limited degree by increasing the equivalent steel thickness of components that are located between the tank armor and the critical components. This effect is discussed in more detail in the following.

The role of the ability of components to provide protection for critical components they may shield is demonstrated to some extent by Fig. 5. In this figure, normalized kill probability is plotted as a function of normalized component equivalent shielding thickness for fragments with the baseline speed (lower curve), and for fragments with four times the baseline speed (upper curve). The figure shows that, for the particular combination of critical component character, relative component placement, number, mass and baseline speed of fragments studied, the normalized component equivalent shielding thickness has significant effect on the kill probability over the range of component equivalent shielding thicknesses considered. As to be expected, kill probability decreases with an increase in component equivalent steel shielding thickness. This decrease is 32% for the lower curve and 14% for the upper curve as $\overline{ET}$ is doubled from 1 to 2. Figure 5 also illustrates that an increase in component equivalent shielding thickness can be employed to offset to some extent the increase in $\bar{P}_k$ due to increased fragment speed. For example, if fragment speed is quadrupled, the $\bar{P}_k$ increases from about .496 (lower curve) to about .864 (upper curve) for a normalized component equivalent shielding thickness equal to one. This is a 74% increase in $\bar{P}_k$. However, if added shielding is provided the critical components by doubling the $\overline{ET}$, the resultant $\bar{P}_k$ is about .74. This is only 49% above the initial value of .496 as compared with the 74% increase that would otherwise occur if the fragment speed were quadrupled without doubling the normalized component equivalent shielding thickness. The net savings then in $\bar{P}_k$ is 15%. This shows that decreased tank kill probability can be achieved by increasing the effective shielding thickness, or ballistic "hardness", of noncritical components placed between the basic tank armor and critical components. It also serves to demonstrate that this effect can be characterized quantitatively by AVVAM-1.

Figure 6 shows the effect of component conditional kill probability on tank kill probability for constant values of the baseline case. As indicated, overall tank kill probability increases with increasing probability that its critical components are killed if they are hit by the behind-the-plate fragments. Over the range of normalized component conditional kill probability from 0.5 to 1.0 the normalized tank kill probability increases 23%. This is a highly significant increase. It is the highest of all the rates of change of normalized kill probability found for variations in the baseline fragment and tank component independent variables studied.

The rate of change of normalized tank kill probability with respect to a particular variable (the slopes of the curves in Figures 2 through 6) indicates the sensitivity of the tank kill probability to the variable. Thus, the relative values of these variations indicate the relative sensitivity of the tank vulnerability to these variables. The following is a list of these variations in order of decreasing value over the range of normalized number of fragments, mass, speed, and component equivalent steel shielding thickness from 1 to 2 and normalized component conditional kill probability from 0.5 to 1, all obtained for the baseline conditions:

$$\frac{d\,\overline{P}_k}{d\,\overline{P}_{K/H}} = 0.186$$

$$\frac{d\,\overline{P}_k}{d\,\overline{ET}} = -0.159$$

$$\frac{d\,\overline{P}_k}{d\,\overline{S}} = 0.123$$

$$\frac{d\,\overline{P}_k}{d\,\overline{N}} = 0.070$$

$$\frac{d\,\overline{P}_k}{d\,\overline{M}} = 0.069$$

From this list it is easily seen for the conditions studied that the tank vulnerability is most sensitive to the characteristics of its components and is least sensitive to the attacking shaped charge behind-the-armor fragment number and mass characteristics. The sensitivity of the tank's vulnerability to its components' characteristics at 0.186 and -0.159 is more than double its sensitivity to the number and mass of fragments produced by the baseline shaped charge munition. Therefore, slight variations in the characteristics of the tank components both in vulnerability to ballistic damage from behind-the-armor fragments and in the ability of noncritical components to provide ballistic shielding for the components critical to the tank's mission can be expected to cause large variations in the tank's overall vulnerability.

This situation may be used to advantage in guiding armored vehicle design. Attention given during the design and selection of critical components to achieving modest increases in vulnerability reduction of these components promises potential for achieving large benefits in reducing the tank's overall vulnerability. This is equally true for selection of and design improvements to components that would increase their resistance to ballistic perforation. Here again modest increases in ballistic perforation resistance (equivalent steel thickness) show the potential for significant gains in reducing tank vulnerability.

On the other hand, since the tank vulnerability is relatively insensitive to variations in both the number and mass of the behind-the-armor fragments, it appears that little is to be gained by concentrating on these factors. Furthermore any gain in this area would require considerable effort. Large reductions in either the number of fragments or their masses are apparently required to cause a significant reduction in the overall vulnerability of the tank studied here.

A more fruitful area for tank vulnerability reduction efforts than controlling the number and mass of fragments is pointed out by the sensitivity results. This area is fragment speed. Since the tank vulnerability is almost as sensitive to fragment speed as it is to the characteristics of its components, significant potential for meaningful vulnerability reduction appears to lie in reducing the speed of behind-the-armor fragments. Therefore, this suggests work should be done on the basic tank armor (if feasible) to reduce the speed of the fragments forced out of the back surface of the armor.

It should be kept in mind that the results obtained in this study and discussed here concern a specific tank, a specific hostile munition, and a limited investigation of a small number of parameters involved in tank vulnerability. It may be possible that the order and degree of the influence of of the variables studied could be widely different under different conditions, that is, if the range of the variables studied were widened or if a narrower range were investigated at extreme ends of the possible spectrum of the variables. In any event, the case presented here provides a sample illustration of the potential applications of AVVAM-1 to weapons systems effectiveness studies and the systems acquisition process.

Summary

A general description of AVVAM-1 (Armored Vehicle Vulnerability Analysis Model - First Version) along with the results of a limited tank vulnerability sensitivity study obtained by use of AVVAM-1 have been presented and discussed. This sensitivity study has been performed and reported here to illustrate, by means of a limited study, the potential applications of this new model to weapons systems effectiveness studies and the systems acquisition process.

References

1. Haskell, D. F. and M. J. Reisinger, "AVVAM-1, Armored Vehicle Vulnerability Analysis Model - First Version", Ballistic Research Laboratories, BRL IMR No. 85, February 1973.

2. "MAGIC Computer Simulation", Volumes I and II, Naval Weapons Center Technical Note 4565-3-71, Vol. I and II, May 1971.

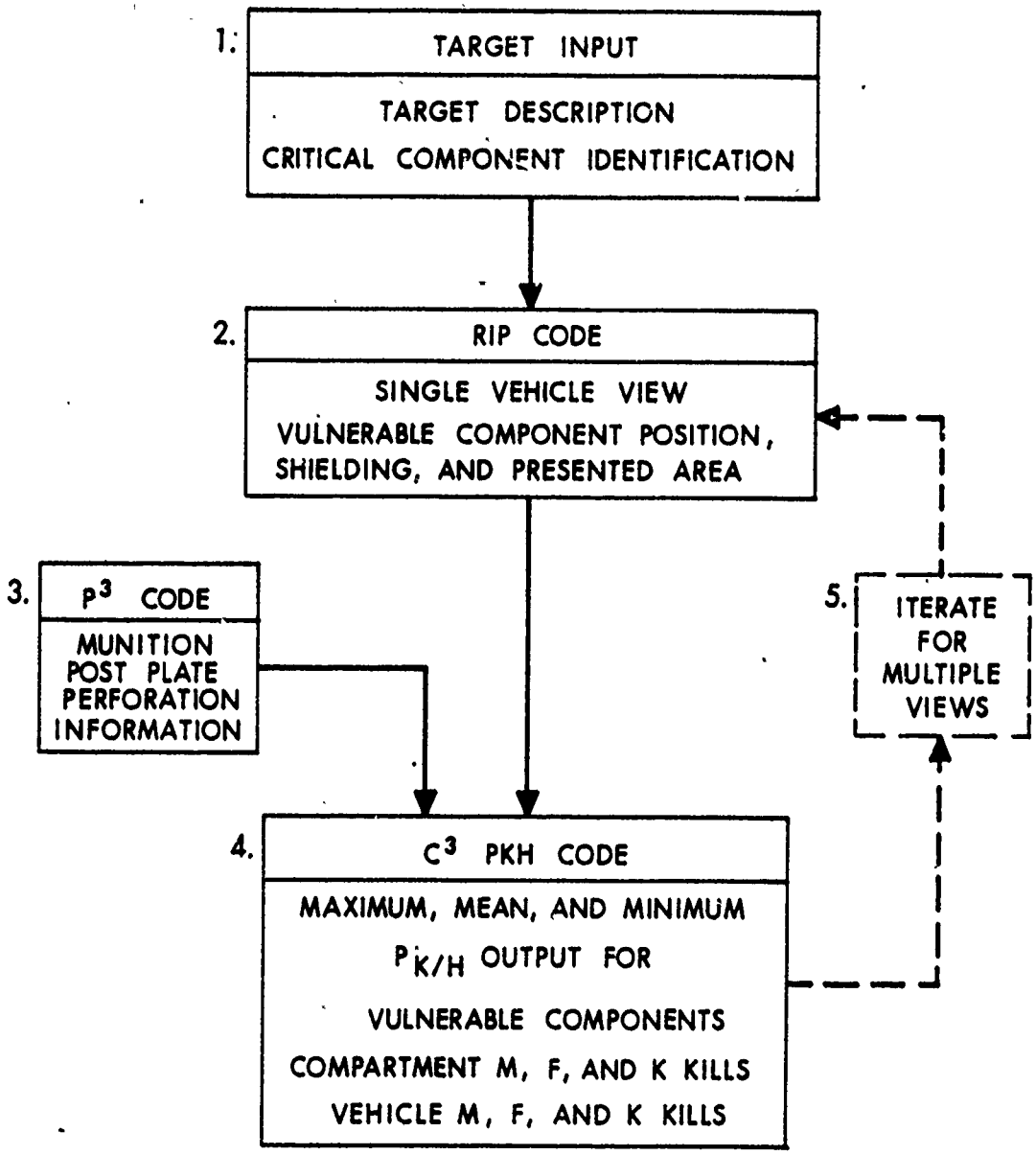


Figure 1. AVVAM-1 Code Summary Flow Chart

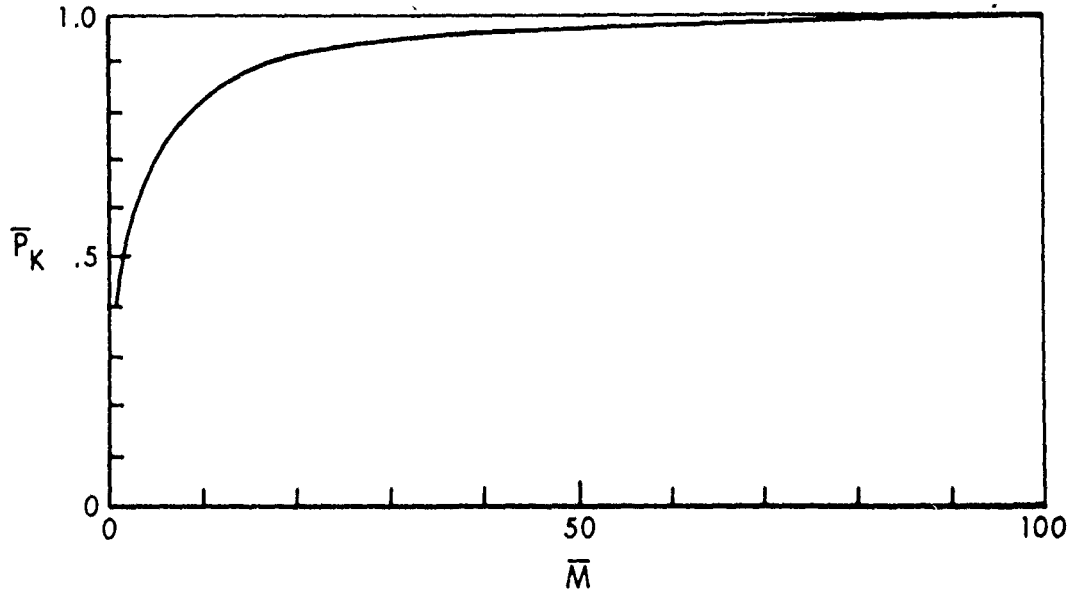


Figure 2. Effect of Normalized Fragment Mass on $\overline{P}_K$

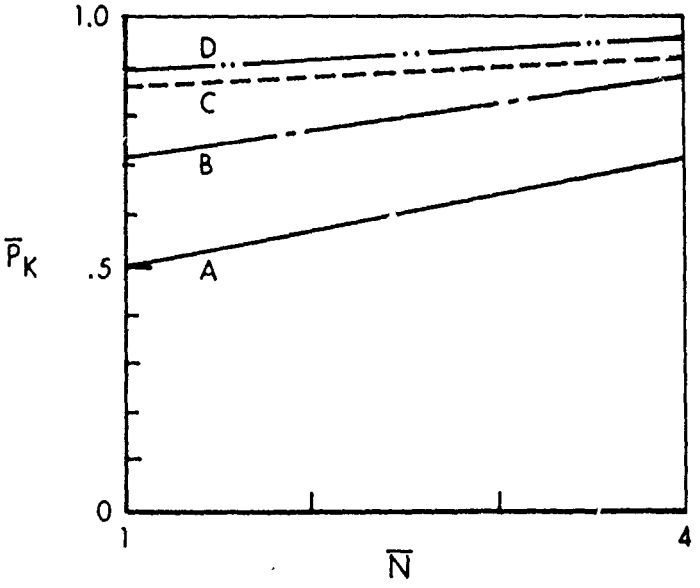


Figure 3. Effect of Normalized Number of Fragments on $\overline{P}_K$.

CURVE A: M, S, ET, PKH
B: 4M, S, ET, PKH
C: M, 4S, ET, PKH
D: 4M, 4S, ET, PKH

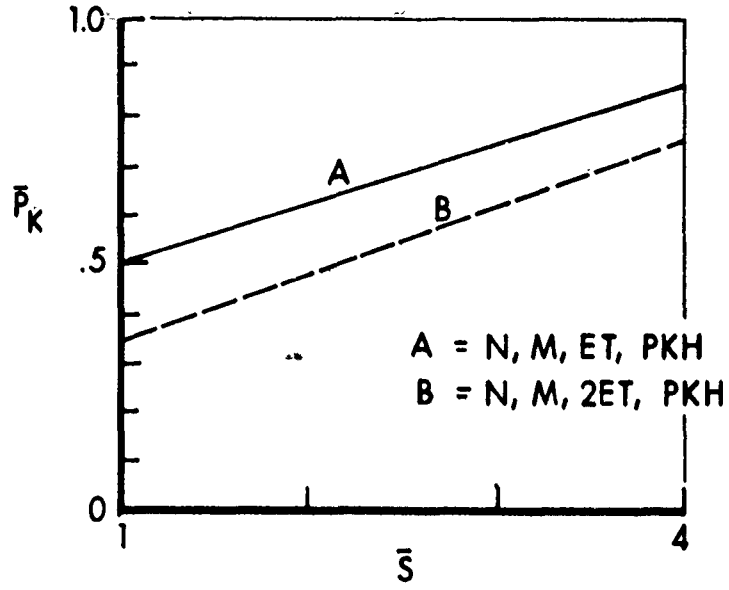


Figure 4. $\bar{P}_K$ Variation with Normalized Fragment Speed

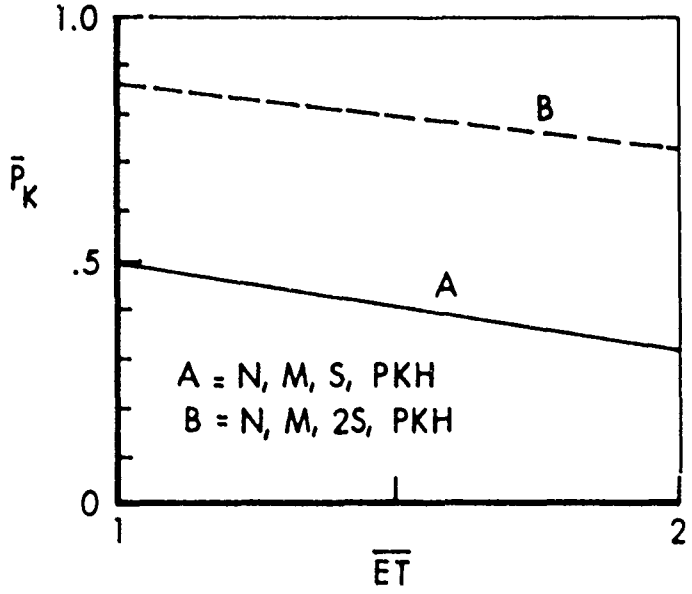


Figure 5. Effect of Normalized Equivalent Shielding Thickness on $\bar{P}_K$

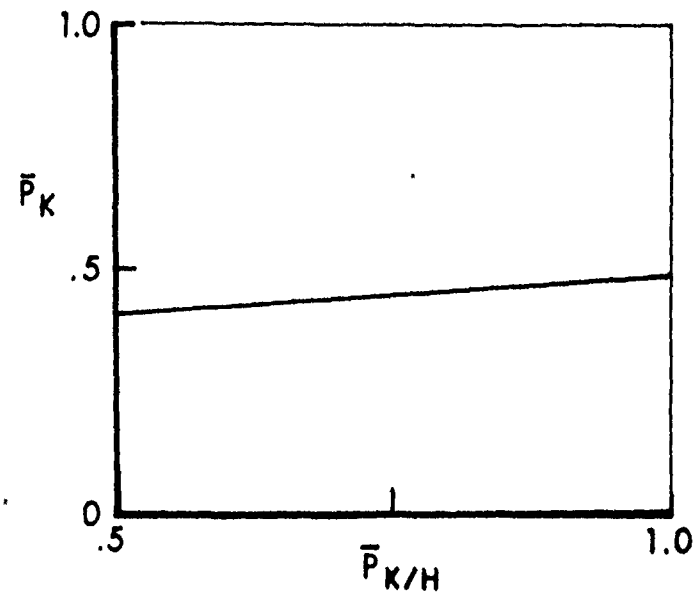


Figure 6. $\bar{P}_K$ Variation with Normalized Component Kill Probability